Published in final edited form as:
Gastroenterology. 2012 March ; 142(3): 543–551.e7. doi:10.1053/j.gastro.2011.11.020.

4-Hydroxy-2-Nonenal Mediates Genotoxicity and Bystander Effects Caused by *Enterococcus faecalis*-Infected Macrophages

Xingmin Wang[1,3], **Yonghong Yang**[1,3], **Danny R. Moore**[1,4], **Susan L. Nimmo**[6], **Stanley A. Lightfoot**[2,5], and **Mark M. Huycke**[1,3,4,*]

[1]The Muchmore Laboratories for Infectious Diseases Research, Research Service, Oklahoma City, OK 73104

[2]Pathology and Laboratory Service, Department of Veterans Affairs Medical Center, Oklahoma City, OK 73104

[3]Department of Radiation Oncology, University of Oklahoma Health Sciences Center, Oklahoma City, OK 73104

[4]Department of Medicine, University of Oklahoma Health Sciences Center, Oklahoma City, OK 73104

[5]Department of Pathology, University of Oklahoma Health Sciences Center, Oklahoma City, OK 73104

[6]Department of Chemistry & Biochemistry, University of Oklahoma, Norman, OK 73019, USA

Abstract

BACKGROUND & AIMS—*Enterococcus faecalis* is a human intestinal commensal that produces extracellular superoxide and promotes chromosome instability via macrophage-induced bystander effects. We investigated the ability of 4-hydroxy-2-nonenal (4-HNE)—a diffusible breakdown product of ω-6 polyunsaturated fatty acids—to mediate these effects.

METHODS—4-HNE was purified from *E faecalis*-infected macrophages; its genotoxicity was assessed in human colon cancer (HCT116) and primary murine colon epithelial (YAMC) cell lines.

RESULTS—4-HNE induced G_2M cell cycle arrest, led to formation γH2AX foci, and disrupted the mitotic spindle in both cell lines. Binucleate tetraploid cells that formed following incubation with 4-HNE were associated with the activation of stathmin and microtubule catastrophe. Silencing glutathione *S*-transferase α-4, a scavenger of 4-HNE, increased susceptibility of epithelial cells to 4-HNE-induced genotoxicity. Interleukin-10 knockout mice colonized with superoxide-producing *E faecalis* developed inflammation and colorectal cancer, whereas colonization with a superoxide-deficient strain resulted in inflammation but not cancer. 4-HNE-protein adducts were found in the lamina propria and macrophages in areas of colorectal inflammation.

Corresponding author: Mark M. Huycke, M.D., Veterans Affairs Medical Center, 921 N.E. 13th Street, Oklahoma City, OK 73104, mark-huycke@ouhsc.edu.

Disclosure: The authors disclose no conflicts of interest.

Author Contributions: Mark M. Huycke and Xingmin Wang: study concept and design, analysis and interpretation of data, writing of the manuscript; Xingmin Wang, Yonghong Yang, Danny R. Moore, and Susan L. Nimmo: acquisition of data; Stanley A. Lightfoot: analysis and interpretation of data.

CONCLUSIONS—4-HNE can act as an autochthonous mitotic spindle poison in normal colonic epithelial and colon cancer cells. This finding links the macrophage-induced bystander effects to colorectal carcinogenesis.

Keywords

CRC model; genetic; cell division; mitosis

Introduction

The intestinal microbiota are necessary to many transgenic models of colorectal cancer (CRC).[1–5] Considerable evidence implicates interactions between commensals and the innate immune system in carcinogenesis[6] with macrophages acting as key effectors in cancer initiation and progression.[7] As specialized cells of the monophagocytic lineage, macrophages are the most abundant antigen-presenting cell in the intestinal lamina propria and an essential component of defense against exogenous pathogens and induction of tolerance to commensals.[8, 9] However, mechanisms by which intestinal microbiota and macrophages elicit transforming events in CRC remain to be defined.

Bystander effects are a feature of macrophage biology that potentially link innate immunity to carcinogenesis.[10, 11] This phenomenon was originally described for cells that were activated by irradiation to generate chromosomal instability (CIN) in neighboring non-irradiated cells. We recently showed that *Enterococcus faecalis*, a human intestinal commensal that causes intestinal inflammation and cancer in interleukin (IL)-10 knockout mice,[1, 2] can activate macrophages through the production of extraceulluar superoxide to generate bystander effects and CIN in adjacent cells.[12, 13] Cyclooxygenase-2 (COX-2) appears integral to both *E. faecalis*- and radiation-induced models of bystander effects,[12, 14] and help link intestinal commensals to inflammation and CRC. The diffusible clastogens that mediate these effects, however, remain to be characterized.

The ability of *E. faecalis* to generate bystander effects derive in part from a unique bacterial phenotype—extracellular superoxide production.[12, 13, 15] *E. faecalis* produces this anionic radical as a byproduct of electron transport through a rudimentary respiratory chain. In the presence of transition metals, superoxide causes lipid peroxidation and can form highly reactive electrophiles such as 4-hydroxy-2-nonenal (4-HNE), malondialdehyde, and 4-oxo-2-nonenal.[16] These α, β-unsaturated aldehydes are diffusible, can covalently modify proteins, and are known to form mutagenic DNA adducts.[17–19] Among these, 4-HNE has been the most intensively studied and may additionally contribute to carcinogenesis by inhibiting DNA repair, inducing COX-2, and modulating MAPK and NF-κB signaling.[20–23] Mammalian cells are protected from toxic aldehydes by glutathione *S*-transferases (GSTs), aldehyde dehydrogenases, and alcohol dehydrogenases.[18] Among these, glutathione *S*-transferase alpha-4 (Gsta4) is a primary inactivating enzyme for 4-HNE. *Gsta4* null mice have increased levels of 4-HNE-protein adducts and show enhanced susceptibility to oxidative stress.[24] In a dual-chamber model for bystander effects, we found depletion of cellular glutathione increased CIN in target cells.[13]

To further investigate 4-HNE as a potential mediator of bystander effects, we measured, and then purified, this electrophile from activated macrophages and tested the ability of 4-HNE to cause DNA damage, promote CIN, and accumulate in the colons of *IL-10*$^{-/-}$ mice colonized with *E. faecalis*. We found that colonic epithelial cells exposed to this purified aldehyde developed γH2AX foci and cell cycle arrest. In addition, 4-HNE treatment damaged the mitotic spindle and caused a failure of cytokinesis that led to tetraploidy. Silencing *Gsta4* exacerbated 4-HNE-induced DNA damage and promoted tetraploidy.

Finally, in *IL-10*$^{-/-}$ mice colonized with *E. faecalis* 4-HNE-protein adducts accumulated in colon macrophages. These findings provide evidence for 4-HNE as an autochthonous spindle poison that links macrophage-induced bystander effects to CRC.

Materials and Methods

Cell lines and bacteria

The near-diploid HCT116 human colon cancer cell (ATCC), YAMC primary mouse colon epithelial cell (Ludwig Institute for Cancer Research, New York), and RAW264.7 murine macrophage cell (ATCC) lines were grown as previously described.[12, 25] *E. faecalis* strain OG1RFSS was spontaneously derived from OG1RF—a Gram-positive human commensal—and expressed high-level resistance to spectinomycin and streptomycin.[26] *menB* was deleted in *E. faecalis* OG1RF and an isogenic derivative WY84SS selected for spontaneous resistance to spectinomycin and streptomycin (see Supplementary Materials and Methods). *menB* encodes 1,4-dihydroxy-2-naphthoic acid synthase. Its inactivation leads to loss of membrane associated demethylmenaquinones and attenuation of extracellular superoxide production by *E. faecalis*.[26] A dual-chamber co-culture system was used to expose colonic epithelial cells to uninfected or *E. faecalis*-infected macrophages as previously described.[12]

Purification and analysis of 4-HNE

RAW264.7 cells were infected with OG1RF at a multiplicity of infection (MOI) of 1,000 colony-forming units (cfu) per macrophage at 37°C for 2 hrs. Supernatants were extracted using a modified Folch procedure and 4-HNE separated by high performance liquid chromatography and analyzed using a 4-cell CoulArray detector (ESA) with voltages set at 100, 150, 200, and 400 mV. 4-HNE purity, concentration, and structure were analyzed by 1-D and 2-D ^{1}H and ^{13}C nuclear magnetic resonance using benzene as an internal control as described in the Supplementary Materials and Methods (Figure S1).

Gsta4 knockdown

Gsta4 expression in YAMC cells was silenced using the BLOCK-iT™ Pol II miR RNAi Expression System (Invitrogen). YAMC cells were transfected with Gsta4 specific RNAi-expressing (pcDNA™6.2-GW/miR) and negative control plasmids according to the manufacturer's instructions.

Colonization of *IL-10*$^{-/-}$ and *IL-10*$^{+/+}$ mice

Specific pathogen- and viral-free *IL-10*$^{-/-}$ knockout and *IL-10*$^{+/+}$ mice (129S6/SvEv, Jackson Laboratory) were colonized with *E. faecalis* OG1RFSS, WY84SS, or sham as previously described.[26] Colonization was maintained using spectinomycin and streptomycin in drinking water. Mice were housed using a biosafety level 3 facility to assure contact and airborne isolation and minimize potential cross-contamination. The genotype of mice was confirmed by PCR as previously described.[27] Biopsies of the rectum, distal, mid, and proximal colon along with ileum, jejunum, and duodenum were obtained at necropsy after colonization for 3 and 9 months. Protocols were approved by the University of Oklahoma Health Sciences Center IACUC and Oklahoma City Department of Veterans Affairs Animal Studies Committee.

Statistical analysis

Data were expressed as means with the standard deviation. Student's *t* test was used for comparison between experimental groups and controls. Analysis of variance was used for multiple comparisons across time for 4-HNE production by macrophages. *P* values < 0.05 were considered significant.

Results

E. faecalis-infected macrophages produce 4-HNE

We initially assayed *E. faecalis*-infected RAW264.7 cells for 4-HNE production and confirmed its structure by 2-D NMR. ^{1}H and ^{13}C shifts were consistent with *trans*-4-hydroxy-2-nonenal (Figure 1*A*). Compared to uninfected controls, RAW264.7 cells infected with OG1RF at an MOI of 1,000 had a 2-fold increase in 4-HNE concentration in supernatants at 24 to 72 hrs post-infection ($P < 0.01$) (Figure 1*B*). No significant increase was noted for supernatants from RAW264.7 cells infected with OG1RF at lower MOIs (100 and 10) or superoxide-deficient strain WY84 at an MOI of 1,000. Of note, 4-HNE concentration was also increased in the supernatants of RAW264.7 cells infected with *E. coli* DH5α at an MOI of 100 ($P < 0.01$) indicating that this effect was not specific for *E. faecalis* (Figure 1*B*), and is consistent with the colitogenic properties of *E. coli*.[1] It was not feasible to measure 4-HNE in RAW264.7 cells at an *E. coli* DH5α MOI of 1,000 as this concentration of bacteria led to cell death. Immunocytochemical staining for 4-HNE-protein adducts showed increased intensity and number of positively stained RAW264.7 cells following infection by OG1RF and WY84 at an MOI of 1,000 compared to controls (Figure 1*C*). This showed that 4-HNE strongly reacted with intracellular protein targets in addition to diffusing out of cells.

4-HNE damages DNA

To investigate mechanisms by which macrophages induce bystander effects, we purified 4-HNE from macrophages and used that in all subsequent experiments. The LD_{50} for 4-HNE for HCT116 and YAMC cells was 5 μM and 2 μM, respectively (Figure S2). Greater than 90% of cells survived exposure to 2.5 μM and 1 μM, respectively, and these lower doses were used in the following experiments.

We initially measured the effect of 4-HNE on cell cycle for HCT116 and YAMC cells synchronized in G_1. FACS analysis showed a G_2M cell cycle arrest in both cell lines 48 hrs post-exposure (Figure 2*A* and *B*). These observations mirrored the G_2M arrest noted by us previously for HCT116 cells exposed to *E. faecalis*-infected macrophages.[13] DNA damage in cells was assessed by measuring γH2AX foci, a marker for DNA double-strand breaks, following 4-HNE treatment. A dose response was observed for HCT116 cells compared to untreated controls (49.2 ± 7.7 percent vs. 8.1 ± 0.3 percent, respectively; $P = 0.02$; Figure 2*C* and *D*). Similar findings were noted for YAMC cells (13.9 ± 1.3 percent treated vs. 7.3 ± 0.2 percent untreated, $P = 0.02$; Figure 2*E* and *F*). These data show that, at non-cytotoxic doses, 4-HNE induces cell cycle arrest and acts as a diffusible clastogen to damage DNA.

4-HNE generates tetraploidy

Previous work by us showed that *E. faecalis*-infected macrophages can generate aneuploidy and tetraploidy in colonic epithelial cells.[13] To investigate whether 4-HNE could mediate these effects, we exposed HCT116 and YAMC cells to non-toxic doses of this aldehyde and found no change in the percentage of cells with aneuploidy. Both cell lines, however, showed increased numbers of tetraploid cells containing two nuclei (Figure 3*A* and 3*B*). For HCT116 cells, tetraploidy increased from 0.21 ± 0.08 percent for untreated controls to 9.90 ± 0.09 percent following 4-HNE treatment ($P<0.001$; Figure 3*A*, *upper* and 3*C*, *left*). Similarly, for YAMC cells tetraploidy increased from 0.12 ± 0.06 for untreated controls to 0.68 ± 0.10 percent for 4-HNE-treated cells ($P<0.001$; Figure 3*A*, *lower* and 3*C*, *right*).

To confirm the specificity of 4-HNE, we substituted it with *trans*-2-nonenal, an aldehyde of identical length but lacking the C_4 hydroxyl moiety required for reactivity.[18] No cytotoxicity was observed at concentrations below 40 μM (Figure S3). Compared to controls, there was

no change in the percent of tetraploid HCT116 and YAMC cells after treatment with *trans*-2- nonenal at 2.5 μM and 1 μM, respectively (Figure 3*A*, *middle* and 3*C*). This led us to conclude that the C_4 hydroxyl group of 4-HNE was essential to the tetraploid-inducing effect of this electrophile.

4-HNE activates stathmin

4-HNE readily reacts with many proteins to modify function and DNA to cause mutations.[18, 28] Following 4-HNE treatment, HCT116 cells showed global modification of cellular proteins using anti-4-HNE-protein adduct antibody (Figure S4*A*). Based on recent reports that 4-HNE can modify tubulins and inhibit microtubule polymerization,[29, 30] we determined whether 4-HNE potentially generates tetraploidy through this mechanism. To evaluate this we treated HCT116 cells with 4-HNE or supernatants from *E. faecalis*-infected macrophages. Laser-scanning confocal microscopy showed marked damage to mitotic spindles of cells that were treated with 4-HNE or supernatants. We also observed lagging chromosomes (Figure 4*A*, *ii* and *v*), anaphase bridging (Figure 4*A*, *iii* and *vi*), and multipolar spindles (Figure 4*A*, *iv*). To determine whether 4-HNE reacted with tubulin to form protein adducts, we isolated these proteins from HCT116 and YAMC cells treated with 4-HNE using α/β-tubulin antibody. Western blots showed tubulin monomers but no dimers (Figure S4*B*). Interestingly, no bands were detected using antibody to 4-HNE-protein adducts, suggesting that, at the non-cytotoxic doses used in these experiments, 4-HNE failed to form 4-HNE-tubulin adducts (Figure S4*C*). These findings led us to reconsider the mechanism by which 4-HNE caused mitotic spindle damage.

We next investigated the potential dysregulation of microtubule dynamics as an explanation for 4-HNE-induced mitotic spindle damage. Stathmin is an important regulatory protein that controls microtubule dynamics during mitosis. The dephosphorylated form of stathmin inhibits microtubule formation by sequestering α/β-tubulin heterodimers as stable ternary complexes and thereby decreases the pool of heterodimers available for polymerization.[31] As cells enter mitosis stathmin is inactivated by phosphorylation at Ser^{16}, Ser^{25}, Ser^{38}, and/or Ser^{63}.[32, 33] The result is release of tubulin heterodimers and increased microtubule formation. Upon completion of mitosis, stathmin is reactivated by dephosphorylation to trigger spindle disassembly (or microtubule catastrophe).[34] When HCT116 and YAMC cells were treated with 4-HNE, the 19 kDa Ser^{16}-phosphorylated form of stathmin decreased substantially at 30 min post-treatment and persisted for 24 hrs (Figure 4*B*, *C*, and S5). In comparison, nocodazole, a prototypical spindle poison, showed small inconsistent changes in this phosphorylated isoform (Figure 4*B*, *C*, and S5). In contrast, the 20 kDa isoform of Ser^{16}-phosphorylated stathmin, one of several multi-phosphorylated isoforms of stathmin,[32] increased in HCT116 cells after exposure to 4-HNE or nocodazole (Figure 4*B* and *D*). Reductions in the 19 and 20 kDa Ser^{16}-phosphorylated forms of stathmin were also evident in YAMC cells at early and late time points following exposure to nocodazole and 4-HNE (Figure S5). The final effect of these changes, *i.e.*, decreases in the key 19 kDa Ser^{16}-phosphorylated isoform of stathmin, was loss of spindle morphology in dividing cells (Figure 4*A*).

In summary, *E. faecalis*-infected macrophages produce increased quantities of 4-HNE, induce G_2M arrest, generate γH2AX foci, and cause tetraploidy in transformed and non-transformed colonic epithelial cells. Spindle dysfunction, tetraploidy, and DNA damage were associated with dephosphorylation of p-stathmin at Ser^{16}. These findings are consistent with 4-HNE acting as a spindle poison to mediate macrophage-induced bystander effects.

Gsta4 enhances 4-HNE catabolism

We next considered whether decreased cellular detoxification of 4-HNE would lead to increased genotoxicity in target cells. Gsta4 is a phase II glutathione *S*-transferase (GST) that detoxifies 4-HNE. We silenced this enzyme in YAMC cells using constitutively expressed RNAi and confirmed a greater than 80% reduction in Gsta4 protein (Figure 5*A*). *Gsta4*-silenced cells showed attenuated 4-HNE decay compared to cells transfected with a negative control plasmid encoding non-targeting miRNA (Figure S6). *Gsta4*-silenced cells showed increased cytotoxicity at 2 and 4 μM 4-HNE compared to controls, confirming the importance of this enzyme in protection against 4-HNE-mediated cytotoxicity. There were no significant changes in cytotoxicity at 1 μM 4-HNE (Figure 5*B*).

Gsta4 decreases 4-HNE genotoxicity

To determine the role of Gsta4 in clastogenesis, we examined *Gsta4*-silenced YAMC cells for γH2AX foci using the dual-chamber co-culture system.[12] No change in γH2AX-positivity was noted by FACS for wild-type cells exposed to *E. faecalis*-infected macrophages (Figure 5*C*), suggesting that adequate defenses against macrophage-generated clastogenesis existed in this primary cell line. γH2AX-positivity increased, however, when *Gsta4*-silenced cells were exposed to *E. faecalis*-infected macrophages compared to non-infected controls (12.7 ± 1.6 percent vs. 8.9 ± 0.6 percent, respectively; $P = 0.02$) (Figure 5*D*).

Next, we exposed *Gsta4*-silenced YAMC cells to purified 4-HNE and found increased γH2AX-positivity compared to wild-type cells (41.8 ± 1.3 percent vs. 24.6 ± 6.5 percent; $P = 0.01$). No increase in γH2AX-positivity was found for cells transfected with a negative control plasmid (Figure 5*E*). Of note, the proportion of γH2AX-positivity in untreated silenced cells was substantially increased compared to untreated wild-type cells (Figure 5*E*), suggesting that knockdown of *Gsta4* increased the susceptibility of YAMC cells to endogenously generated DNA damage.

Finally, the proportion of tetraploid cells significantly increased following 4-HNE treatment in *Gsta4*-silenced YAMC cells compared to wild-type controls (0.96 ± 0.18 percent vs. 0.65 ± 0.11 percent, respectively; $P = 0.03$). The percentage of tetraploid cells transfected with the negative control plasmid was 0.70 ± 0.08 and similar to wild-type cells ($P = 0.98$) (Figure 5*F*). These data indicate that silencing *Gsta4* in YAMC cells attenuates 4-HNE decay, exacerbates 4-HNE-induced DNA damage, and promotes tetraploidy. Together, these findings are consistent with 4-HNE acting as a mediator for macrophage-induced bystander effects.

E. faecalis generates 4-HNE-protein adducts

IL-10$^{-/-}$ mice were colonized with a superoxide-producing *E. faecalis* strain OG1RFSS, a superoxide-deficient strain WY84SS, or administered sham. *IL-10*$^{+/+}$ control mice were colonized with OG1RFSS. Throughout the study, colonization of mice by OG1RFSS and WY84SS remained between 0.5 and 1.0 × 10^9 colony-forming units per gram feces with no differences between these groups. Histopathological findings in the large intestine were limited to the distal colon and rectum. Although inflammation was evident after 3 months of colonization, there was no significant difference in inflammation scores or evidence of severe dysplasia or cancer (Figure 6*A*). However, after 9 months of colonization, 4 of 7 *IL-10*$^{-/-}$ OG1RFSS mice had developed cancer compared to 0 of 11 *IL-10*$^{-/-}$ WY84SS mice (Figure 6*A* and *B*; P = 0.01). Sham-treated *IL-10*$^{-/-}$ mice, and wild-type mice colonized with OG1RFSS, did not develop inflammation or cancer. Immunohistochemical analyses using anti-4-HNE-protein adduct antibody showed staining of colonic macrophages and myofibroblasts in *IL-10*$^{-/-}$ mice colonized with OG1RFSS (Figure 6*C*). 4-HNE-protein

adducts staining was minimal or not visible in colonic macrophages for knockout mice colonized with WY84SS or administered sham or for wild-type mice colonized with OG1RFSS (Figure 6*D* and *E*).

Discussion

We previously reported that *E. faecalis*-infected macrophages generate bystander effects that cause G_2M cell cycle arrest and CIN in epithelial cells.[12, 13] In this study we demonstrate that bystander effects induced by *E. faecalis* are associated with increased production of 4-HNE by infected macrophages. This aldehyde is a breakdown product of lipid peroxidation[16] and acts as a diffusible clastogen[19] that causes γH2AX deposition due to DNA double-strand breaks. It also induces G_2M cell cycle arrest and damages the mitotic spindle. One additional consequence of 4-HNE exposure was the development of tetraploidy in both transformed and primary colon epithelial cells. γH2AX deposition noted in this study most likely represented DNA double-strand breaks since we previously found *E. faecalis*-induced DNA damage in colonic epithelial cells using the comet assay.[26] Finally, colonization of *IL-10*$^{-/-}$ mice with wild-type *E. faecalis* that produces extracellular superoxide, compared to a demethylmenaquinone-deficient and superoxide-attenuated Δ*menB* strain, confirmed the role of this radical anion in promoting colorectal carcinogenesis. These observations are also concordant with increased rates of CIN due to superoxide producing *E. faecalis* that we previously noted using the dual-chamber model of macrophage-induced bystander effects.[12, 13]

Since publication of Boveri's treatise on abnormal chromosome number and the origin of malignant tumors,[35] chromosomal missegregation has remained a leading hypothesis for somatic tumorigenesis, in part because numerous observations show both tetraploid and aneuploid cells as common features in most tumors. The mechanisms leading to aneuploidy, however, are likely multiple with tetraploidy recognized as a distinct pathway to aneugenesis.[36] We found that exposure of cells to purified 4-HNE produced binucleate daughter cells. We suspect that this occurred through a failure of cytokinesis and not mitotic slippage since examination of the mitotic spindle by immunoflorescence showed extensive damage.[36] Microtubules are essential to normal cytokinesis and defects in the spindle apparatus have been associated with CIN in oral and gastrointestinal cancers.[37, 38] 4-HNE is a reactive electrophile that, at high concentrations, can directly damage tubulins and microtubules.[29, 30] In this study, 4-HNE treatment of purified tubulins spontaneously generated tubulin dimers (Figure S7). However, we were unable to detect 4-HNE-tubulin adducts in cells exposed to non-cytotoxic doses of 4-HNE.

We therefore considered other mechanisms to explain the failure of cytokinesis and generation of tetraploid cells we observed in vitro. What we discovered was the dephosphorylation of stathmin, or oncoprotein 18 (Op18), a key regulator of microtubule dynamics, in cells exposed to 4-HNE. Stathmin activation during mitosis promotes microtubular depolymerization and can lead to anaphase bridging, lagging chromosomes, cytokinesis failure, and aneuploidy or tetraploidy. Each of these abnormalities has been noted for macrophage-induced bystander effects.[12, 13]

In our experiments, a single dose of purified 4-HNE generated tetraploid cells. In contrast, in a prior study by us using epithelial cells exposed to *E. faecalis*-infected macrophages, we found that the bystander effect led to tetraploidy and aneuploidy,[13] something not observed following 4-HNE treatment. Perhaps other, as yet uncharacterized, aneugenic factors are produced by activated macrophages that promote aneuploidy. Alternately, aneugenesis might require continuous exposure to 4-HNE, and might not be seen following a single dose as was used in these experiments. In any event, purified 4-HNE caused tetraploidization.

This change alone is an important step toward oncogenic transformation since tetraploid cells can become aneuploid and express CIN.[36]

Stathmin is phosphorylated during mitosis by CaMKIV or cAMP-dependent kinases at Ser^{16} or Ser^{63} with a subsequent reduction in tubulin sequestering activity.[31, 39] Although we did not assess the phosphorylation of stathmin at Ser^{25} or Ser^{38}, we note that Cdk1, a kinase responsible for stathmin phosphorylation at these sites,[39, 40] is down-regulated by *E. faecalis*-infected macrophages.[13] Reduction in Cdk1 would lead to the activation of stathmin and potentially contribute to a G_2M cell cycle arrest. Our findings might be due to the modulation of kinases by 4-HNE, but this will require further investigation. In summary, our results indicate that non-cytotoxic doses of 4-HNE can act as a spindle poison and generate tetraploidy through the failure of cytokinesis.

The role of glutathione *S*-transferases in protecting against intestinal inflammation and carcinogenesis is not well defined. *Gsta4* null mice accumulate 4-HNE-protein adducts and show greater susceptibility to bacterial infection and oxidative stress, suggesting a pivotal role for this enzyme in detoxifying peroxidation products.[24] Selective overexpression of *Gsta4* led to decreased inflammation in conventional and germfree mice with dextran sulfate sodium-induced colitis.[41] A recent study using *Gstp* null $Apc^{Min/+}$ mice showed significantly decreased survival, a 6-fold increase in the incidence of colon adenomas, and a 50-fold increase in adenoma multiplicity compared to *Gstp* wild-type $Apc^{Min/+}$ mice.[42] However, there are no reports that associate GSTA4 with an altered risk for cancer in humans. Considering the genotoxic potential of endogenously produced 4-HNE, additional study into the role of GSTA4 in cancer is needed.

In summary, our findings show that *E. faecalis*-infected macrophages produce 4-HNE. This electrophile, when purified, mediated bystander effects in colonic epithelial cells by generating γH2AX foci and inducing G_2M cell cycle arrest. 4-HNE was also associated with mitotic spindle damage, activation of stathmin, cytokinesis failure, and the development of tetraploidy. Silencing *Gsta4* led to increased 4-HNE genotoxicity in target cells. Finally, wild-type *E. faecalis* triggered carcinogenic events in $IL\text{-}10^{-/-}$ mice. 4-HNE-protein adducts were predominant in colon macrophages in these mice. Mice colonized with an isogenic demethylmenaquinone-deficient and superoxide-attenuated strain of *E. faecalis* developed colitis but not cancer. In aggregate, these results show that 4-HNE can act as an autochthonous spindle poison and link macrophage-induced bystander effects to CRC.

Supplementary Material

Refer to Web version on PubMed Central for supplementary material.

Acknowledgments

This study was supported by grants CA127893 (M. M. Huycke), OCAST HR10-032 (X. Wang), NSF 0639199 (S. L. Nimmo), and funds from the Frances Duffy Endowment. We thank Jim Henthorn in the Flow Cytometry Laboratory and the Rodent Barrier Facility at the University of Oklahoma Health Sciences Center, Robert Whitehead of Vanderbilt University for YAMC cells, and Graça Dores for helpful discussions.

Abbreviations

4-HNE	4-hydroxy-2-nonenal
CRC	colorectal cancer
MOI	multiplicity of infection

cfu	colony-forming units
***IL*-10**	interleukin-10
***Gsta*4**	glutathione *S*-transferase alpha 4
CIN	chromosomal instability
COX-2	Cyclooxygenase-2

References

1. Kim SC, Tonkonogy SL, Albright CA, Tsang J, Balish EJ, Braun J, Huycke MM, Sartor RB. Variable phenotypes of enterocolitis in IL-10 deficient mice monoassociated with two different commensal bacteria. Gastroenterology. 2005; 128:891–906. [PubMed: 15825073]
2. Balish E, Warner T. *Enterococcus faecalis* induces inflammatory bowel disease in interleukin-10 knockout mice. Am J Pathol. 2002; 160:2253–2257. [PubMed: 12057927]
3. Chu F-F, Esworthy RS, Chu PG, Longmate JA, Huycke MM, Wilczynski S, Doroshow JH. Bacteria-induced intestinal cancer in mice with disrupted *Gpx1* and *Gpx2* genes. Cancer Res. 2004; 64:962–968. [PubMed: 14871826]
4. Kado S, Uchida K, Funabashi H, Iwata S, Nagata Y, Ando M, Onoue M, Matsuoka Y, Ohwaki M, Morotomi M. Intestinal microflora are necessary for development of spontaneous adenocarcinoma of the large intestine in T-cell receptor beta chain and p53 double-knockout mice. Cancer Res. 2001; 61:2395–2398. [PubMed: 11289103]
5. Maggio-Price L, Treuting P, Bielefeldt-Ohmann H, Seamons A, Drivdahl R, Zeng W, Lai L, Huycke M, Phelps S, Brabb T, Iritani BM. Bacterial infection of *Smad3/Rag2* double-null mice with transforming growth factor-beta dysregulation as a model for studying inflammation-associated colon cancer. Am J Pathol. 2009; 174:317–29. [PubMed: 19119184]
6. Karin M, Lawrence T, Nizet V. Innate immunity gone awry: linking microbial infections to chronic inflammation and cancer. Cell. 2006; 124:823–35. [PubMed: 16497591]
7. Qian BZ, Pollard JW. Macrophage diversity enhances tumor progression and metastasis. Cell. 2010; 141:39–51. [PubMed: 20371344]
8. Mowat AM. Anatomical basis of tolerance and immunity to intestinal antigens. Nat Rev Immunol. 2003; 3:331–41. [PubMed: 12669023]
9. Lee SH, Starkey PM, Gordon S. Quantitative analysis of total macrophage content in adult mouse tissues. Immunochemical studies with monoclonal antibody F4/80. J Exp Med. 1985; 161:475–89. [PubMed: 3973536]
10. Coates PJ, Rundle JK, Lorimore SA, Wright EG. Indirect macrophage responses to ionizing radiation: implications for genotype-dependent bystander signaling. Cancer Res. 2008; 68:450–6. [PubMed: 18199539]
11. Lorimore SA, Chrystal JA, Robinson JI, Coates PJ, Wright EG. Chromosomal instability in unirradiated hemaopoietic cells induced by macrophages exposed in vivo to ionizing radiation. Cancer Res. 2008; 68:8122–6. [PubMed: 18829571]
12. Wang X, Huycke MM. Extracellular superoxide production by *Enterococcus faecalis* promotes chromosomal instability in mammalian cells. Gastroenterology. 2007; 132:551–61. [PubMed: 17258726]
13. Wang X, Allen TD, May RJ, Lightfoot S, Houchen CW, Huycke MM. *Enterococcus faecalis* induces aneuploidy and tetraploidy in colonic epithelial cells through a bystander effect. Cancer Res. 2008; 68:9909–17. [PubMed: 19047172]
14. Zhou H, Ivanov VN, Gillespie J, Geard CR, Amundson SA, Brenner DJ, Yu Z, Lieberman HB, Hei TK. Mechanism of radiation-induced bystander effect: role of the cyclooxygenase-2 signaling pathway. Proc Natl Acad Sci USA. 2005; 102:14641–14646. [PubMed: 16203985]
15. Huycke MM, Moore D, Joyce W, Wise P, Shepard L, Kotake Y, Gilmore MS. Extracellular superoxide production by *Enterococcus faecalis* requires demethylmenaquinone and is attenuated by functional terminal quinol oxidases. Mol Microbiol. 2001; 42:729–40. [PubMed: 11722738]

16. Catalá A. Lipid peroxidation of membrane phospholipids generates hydroxy-alkenals and oxidized phospholipids active in physiological and/or pathological conditions. Chem Phys Lipids. 2009:157. [PubMed: 19900429]
17. Chung FL, Nath RG, Ocando J, Nishikawa A, Zhang L. Deoxyguanosine adducts of *t*-4-hydroxy-2-nonenal are endogenous DNA lesions in rodents and humans: detection and potential sources. Cancer Res. 2000; 60:1507–1511. [PubMed: 10749113]
18. Uchida K. 4-Hydroxy-2-nonenal: a product and mediator of oxidative stress. Prog Lipid Res. 2003; 42:318–343. [PubMed: 12689622]
19. Emerit I, Garban F, Vassy J, Levy A, Filipe P, Freitas J. Superoxide-mediated clastogenesis and anticlastogenic effects of exogenous superoxide dismutase. Proc Natl Acad Sci USA. 1996; 93:12799–12804. [PubMed: 8917499]
20. Feng Z, Hu W, Tang MS. *Trans*-4-hydroxy-2-nonenal inhibits nucleotide excision repair in human cells: a possible mechanism for lipid peroxidation-induced carcinogenesis. Proc Natl Acad Sci USA. 2004; 101:8598–8602. [PubMed: 15187227]
21. Liu W, Kato M, Itoigawa M, Murakami H, Yajima M, Wu J, Ishikawa N, Nakashima I. Distinct involvement of NF-kappaB and p38 mitogen-activated protein kinase pathways in serum deprivation-mediated stimulation of inducible nitric oxide synthase and its inhibition by 4-hydroxynonenal. J Cell Biochem. 2001; 83:271–80. [PubMed: 11573244]
22. Zarrouki B, Soares AF, Guichardant M, Lagarde M, Geloen A. The lipid peroxidation end-product 4-HNE induces COX-2 expression through p38MAPK activation in 3T3-L1 adipose cell. FEBS Lett. 2007; 581:2394–400. [PubMed: 17481611]
23. Sharma A, Sharma R, Chaudhary P, Vatsyayan R, Pearce V, Jeyabal PV, Zimniak P, Awasthi S, Awasthi YC. 4-Hydroxynonenal induces p53-mediated apoptosis in retinal pigment epithelial cells. Arch Biochem Biophys. 2008; 480:85–94. [PubMed: 18930016]
24. Engle MR, Singh SP, Czernik PJ, Gaddy D, Montague DC, Ceci JD, Yang Y, Awasthi S, Awasthi YC, Zimniak P. Physiological role of mGSTA4–4, a glutathione *S*-transferase metabolizing 4-hydroxynonenal: generation and analysis of *mGsta4* null mouse. Toxicol Appl Pharmacol. 2004; 194:296–308. [PubMed: 14761685]
25. Whitehead RH, VanEeden PE, Noble MD, Ataliotis P, Jat PS. Establishment of conditionally immortalized epithelial cell lines from both colon and small intestine of adult H-2Kb-tsA58 transgenic mice. Proc Natl Acad Sci USA. 1993; 90:587–91. [PubMed: 7678459]
26. Huycke MM, Abrams V, Moore DR. *Enterococcus faecalis* produces extracellular superoxide and hydrogen peroxide that damages colonic epithelial cell DNA. Carcinogenesis. 2002; 23:529–36. [PubMed: 11895869]
27. Czarneski J, Lin YC, Chong S, McCarthy B, Fernandes H, Parker G, Mansour A, Huppi K, Marti GE, Raveche E. Studies in NZB IL-10 knockout mice of the requirement of IL-10 for progression of B-cell lymphoma. Leukemia. 2004; 18:597–606. [PubMed: 14712288]
28. Schaur RJ. Basic aspects of the biochemical reactivity of 4-hydroxynonenal. Mol Aspects Med. 2003; 24:149–59. [PubMed: 12892992]
29. Stewart BJ, Doorn JA, Petersen DR. Residue-specific adduction of tubulin by 4-hydroxynonenal and 4-oxononenal causes cross-linking and inhibits polymerization. Chem Res Toxicol. 2007; 20:1111–9. [PubMed: 17630713]
30. Kokubo J, Nagatani N, Hiroki K, Kuroiwa K, Watanabe N, Arai T. Mechanism of destruction of microtubule structures by 4-hydroxy-2-nonenal. Cell Struct Funct. 2008; 33:51–9. [PubMed: 18360009]
31. Steinmetz MO. Structure and thermodynamics of the tubulin-stathmin interaction. J Struct Biol. 2007; 158:137–47. [PubMed: 17029844]
32. Gavet O, Ozon S, Manceau V, Lawler S, Curmi P, Sobel A. The stathmin phosphoprotein family: intracellular localization and effects on the microtubule network. J Cell Sci. 1998; 111:3333–46. [PubMed: 9788875]
33. Manna T, Thrower DA, Honnappa S, Steinmetz MO, Wilson L. Regulation of microtubule dynamic instability in vitro by differentially phosphorylated stathmin. J Biol Chem. 2009; 284:15640–9. [PubMed: 19359244]

34. Rubin CI, Atweh GF. The role of stathmin in the regulation of the cell cycle. J Cell Biochem. 2004; 93:242–50. [PubMed: 15368352]
35. Boveri, T. Concerning the Origin of Malignant Tumors. The Company of Biologists Limited and Cold Spring Harbor Laboratory Press; 2008. p. 1-82.
36. Storchova Z, Kuffer C. The consequences of tetraploidy and aneuploidy. J Cell Sci. 2008; 121:3859–66. [PubMed: 19020304]
37. Saunders WS, Shuster M, Huang X, Gharaibeh B, Enyenihi AH, Petersen I, Gollin SM. Chromosomal instability and cytoskeletal defects in oral cancer cells. Proc Natl Acad Sci USA. 2000; 97:303–8. [PubMed: 10618413]
38. Green RA, Kaplan KB. Chromosome instability in colorectal tumor cells is associated with defects in microtubule plus-end attachments caused by a dominant mutation in APC. J Cell Biol. 2003; 163:949–61. [PubMed: 14662741]
39. Holmfeldt P, Sellin ME, Gullberg M. Predominant regulators of tubulin monomer-polymer partitioning and their implication for cell polarization. Cell Mol Life Sci. 2009; 66:3263–76. [PubMed: 19585080]
40. Beretta L, Dubois MF, Sobel A, Bensaude O. Stathmin is a major substrate for mitogen-activated protein kinase during heat shock and chemical stress in HeLa cells. Eur J Biochem. 1995; 227:388–95. [PubMed: 7851413]
41. Edalat M, Mannervik B, Axelsson LG. Selective expression of detoxifying glutathione transferases in mouse colon: effect of experimental colitis and the presence of bacteria. Histochem Cell Biol. 2004; 122:151–9. [PubMed: 15309552]
42. Ritchie KJ, Walsh S, Sansom OJ, Henderson CJ, Wolf CR. Markedly enhanced colon tumorigenesis in Apc(Min) mice lacking glutathione S-transferase Pi. Proc Natl Acad Sci U S A. 2009; 106:20859–64. [PubMed: 19915149]

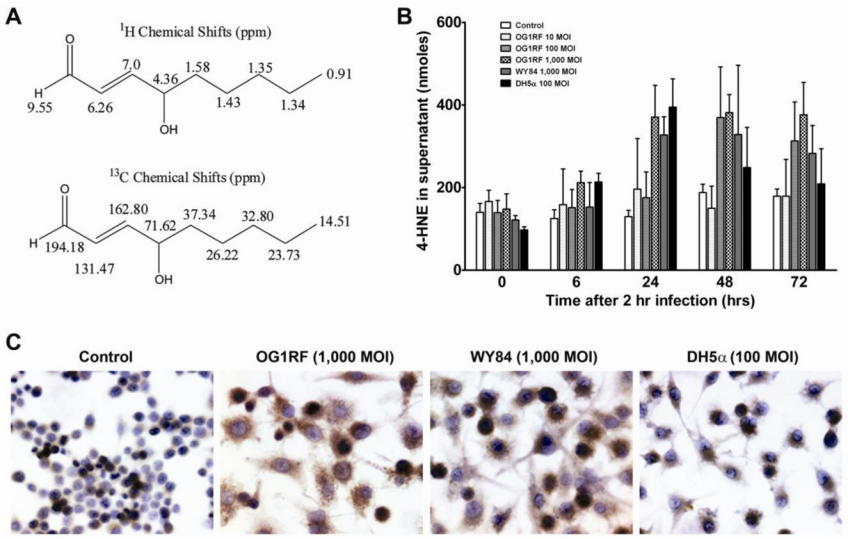

Figure 1. *E. faecalis*-infected macrophages produce 4-HNE

A, 2-D NMR shows 4-HNE from *E. faecalis*-infected macrophages was pure with predicted structure. ^{1}H chemical shifts (*upper*) and ^{13}C chemical shifts (*lower*). *B*, 4-HNE in supernatants of RAW264.7 cells treated with OG1RF at an MOI of 1,000 (checkered) significantly increases from 24–72 hrs post-treatment compared to untreated control ($P<0.01$, white). No significant changes are seen for cells treated with OG1RF at MOIs of 10 ($P=0.6$, stippled), 100 ($P=0.1$, hashed), and WY84 at an MOI of 1,000 ($P=0.08$, gray). Of note, 4-HNE significantly increases in supernatants from RAW264.7 cells treated with *E. coli* DH5α at an MOI of 100 ($P<0.01$, solid). *C*, Immunocytochemical staining for 4-HNE-protein adducts qualitatively shows intracellular accumulation at 48 hrs for RAW264.7 cells treated with OG1RF and WY84 at an MOI of 1,000. No increased staining is noted for cells treated with DH5α at an MOI of 100 compared to an untreated control.

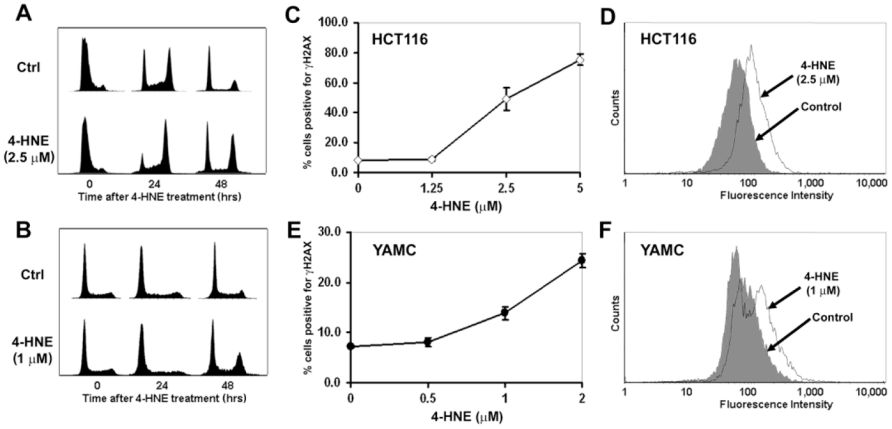

Figure 2. 4-HNE damages DNA

A and *B*, HCT116 (*A*) and YAMC (*B*) cells were synchronized to G_1 and treated with 4-HNE. FACS analysis shows G_2M arrest 48 hrs post-treatment for both cell lines. *C–F*, Exposure of HCT116 (*C*) and YAMC (*E*) cells to 4-HNE generates γH2AX foci in dose-dependent manner. FACS analyses show γH2AX positivity in HCT116 (*D*) and YAMC (*F*) cells following 4-HNE treatment. Filled trace, untreated control; open trace, 4-HNE treatment.

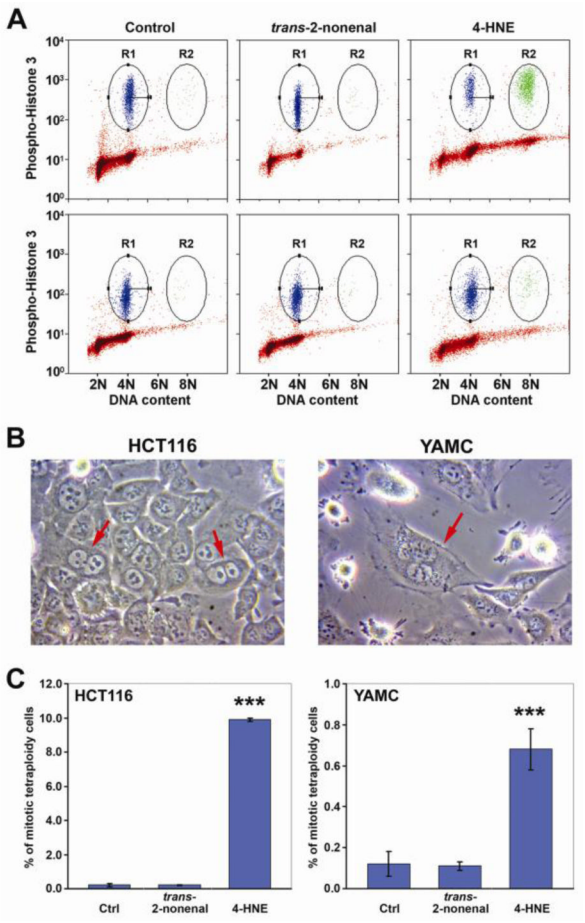

Figure 3. 4-HNE generates tetraploidy

A, FACS analyses for ploidy of HCT116 (*Upper panels*) and YAMC (*Lower panels*) cells following exposure to control (*left*), *trans*-2-nonenal (*middle*), and 4-HNE (*right*). R1, phospho-histone H3-positive cells with 4N DNA content (mitotic diploid cells); R2, phospho-histone H3-positive cells with 8N DNA content (mitotic tetraploid cells). *B*, Exposure of cells to 4-HNE produces double nuclei in HCT116 (*left*) and YAMC (*right*) cells. *C*, 4-HNE-treated HCT116 (*left*) and YAMC (*right*) cells develop tetraploidy (***$P <$ 0.001); *trans*-2-nonenal without effect.

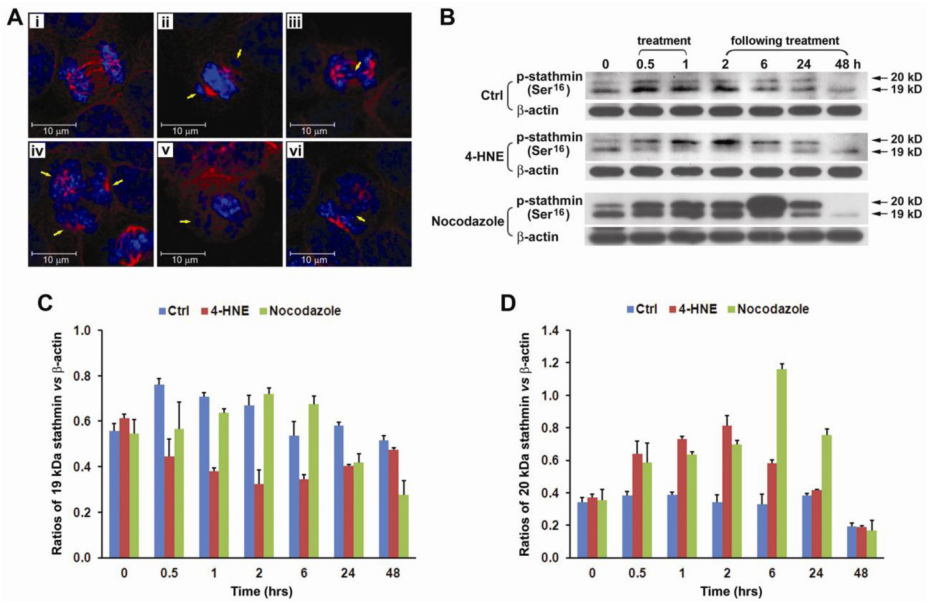

Figure 4. 4-HNE activates stathmin

A, Laser scanning confocal microscopy shows normal microtubules (red) in untreated HCT116 cells (*i*) and degraded microtubules in cells treated with supernatants from *E. faecalis*-infected macrophages (*ii–iv*) or purified 4-HNE (*v* and *vi*); blue represents DNA stain. Treated cells contain lagging chromosomes (*ii*), anaphase bridging (*iii* and *vi*), multipolar spindle (*iv*), and spindle failure at metaphase (*v*). *B*, Western blots show changes in two isoforms (19 and 20 kDa) of p-stathmin (Ser^{16}) in HCT116 cells treated with 4-HNE and nocodazole. *C*, By normalizing to β-actin, the 19 kDa isoform significantly decreases 0.5–6 hrs following 4-HNE treatment (*red*) compared to untreated control (*blue*). This decrease occurs 24 hrs after nocodazole treatment (*green*). *D*, The 20 kDa isoform increases in cells treated with 4-HNE or nocodazole.

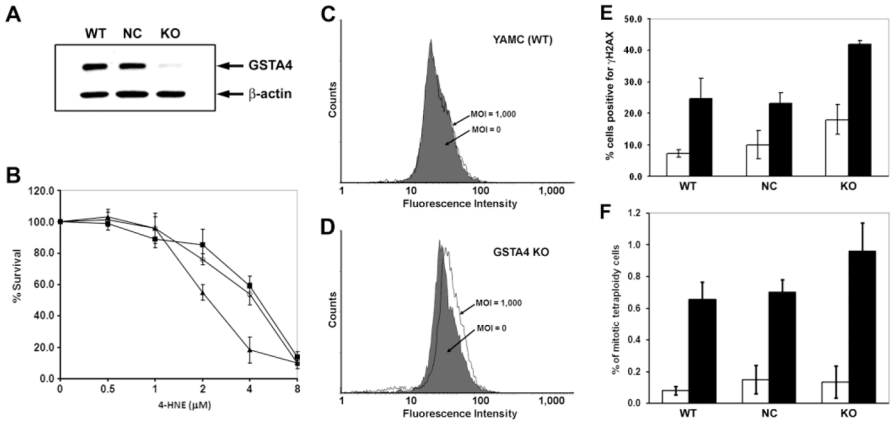

Figure 5. Silencing *Gsta4* increases cell susceptibility to 4-HNE induced genotoxicity

A, Western blot shows >80% reduction in Gsta4 in silenced YAMC cells (KO) compared with wild-type (WT) cells or cells transfected with a negative control plasmid (NC). *B*, Decreased survival for KO cells (*triangle*) exposed to 4-HNE compared with WT cells (*open circle*) or NC cells (*closed square*). *C*, Wild-type YAMC cells exposed to *E. faecalis*-infected RAW264.7 cells for 48 hrs in a dual-chamber co-culture system show no effect on γH2AX-positivity. *Filled trace*, cells exposed to uninfected RAW264.7 cells (MOI = 0); *open trace*, cells exposed to *E. faecalis*-infected macrophages (MOI = 1000). *D*, Increased γH2AX-positivity is noted for *Gsta4*-silenced YAMC cells ($P = 0.02$, MOI of 1,000 vs. 0). *E*, The percentage of γH2AX-positive cells increases for Gsta4-silenced YAMC cells exposed to 4-HNE compared to wild-type YAMC cells ($P = 0.01$). No change was noted for cells transfected with a negative control plasmid (NC) compared to WT ($P = 0.7$). *F*, The percent tetraploid cells increases for KO cells treated with 4-HNE compared to WT cells ($P = 0.03$). No significant change for NC cells ($P = 0.98$). White bar: untreated control; black bar: cells treated with 4-HNE.

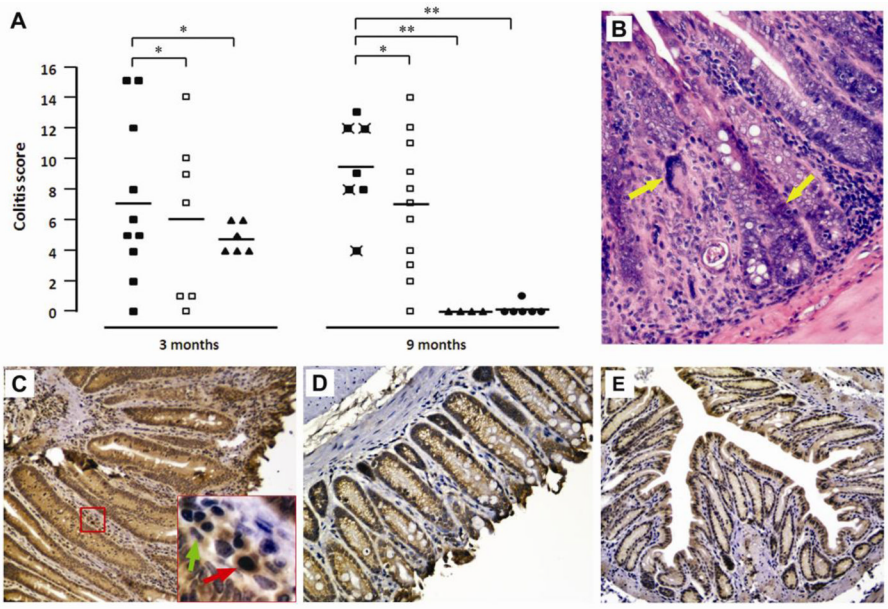

Figure 6. 4-HNE-protein adducts in colon biopsies of *IL-10*$^{-/-}$ mice colonized with *E. faecalis*

A, Histopathological examination and inflammation scores for colorectal biopsies from *IL-10*$^{-/-}$ mice colonized with *E. faecalis* OG1RFSS (closed squares), WY84SS (open squares), or sham (triangles), and *IL-10*$^{+/+}$ mice colonized with OG1RFSS (circles). Biopsies were collected after 3 and 9 months of colonization. Crossed symbols indicate biopsies showing cancer. Biopsies were scored from 0 (low) to 4 (high) on total number of inflammatory cells, decrease in goblet cells, crypt lengthening, reactive atypia, and dysplasia; values were summed for total colitis scores with means shown (bars). *$P > 0.05$; **$P < 0.05$; ***$P < 0.001$. *B*, H&E staining showing cancer in a colon section from an *IL-10*$^{-/-}$ mouse colonized with OG1RFSS. *C*, Immunohistochemical staining of colon biopsy for 4-HNE-protein adducts from *IL-10*$^{-/-}$ mice colonized with OG1FRSS (red arrow, tissue macrophage; green arrow, myofibroblast). *D* and *E*, Minimal or negative staining for 4-HNE-protein adducts in lamina propria of colon biopsies from WY84SS (*D*) or sham-treated *IL-10*$^{-/-}$ mice (*E*).